



Localization and Throughput Trade-Off in a Multi-User Multi-Carrier mm-Wave System

Downloaded from: <https://research.chalmers.se>, 2026-04-05 19:06 UTC

Citation for the original published paper (version of record):

Koirala, R., Denis, B., Uguen, B. et al (2019). Localization and Throughput Trade-Off in a Multi-User Multi-Carrier mm-Wave System. *IEEE Access*, 7: 167099-167112.
<http://dx.doi.org/10.1109/ACCESS.2019.2953777>

N.B. When citing this work, cite the original published paper.

© 2019 IEEE. Personal use of this material is permitted. Permission from IEEE must be obtained for all other uses, in any current or future media, including reprinting/republishing this material for advertising or promotional purposes, or reuse of any copyrighted component of this work in other works.

Date of publication xxxx 00, 0000, date of current version 06/11/2019.

Digital Object Identifier 10.1109/ACCESS.2017.DOI

Localization and Throughput Trade-off in a Multi-User Multi-Carrier mm-Wave System

REMUN KOIRALA^{1,2,3}, BENOÎT DENIS¹, BERNARD UGUEN³, DAVIDE DARDARI², and HENK WYMEERSCH⁴.

¹CEA-Leti Minatec Campus, 17 rue des Martyrs, 38054 Grenoble Cedex 09, France

²DEI-CNIT, University of Bologna, via dell'Università 52, I-47521 Cesena (FC), Italy

³University of Rennes 1-IETR (CNRS UMR 6164), Av. du General Leclerc, 35042, Rennes, France

⁴Department of Electrical Engineering, Chalmers University of Technology, Gothenburg, Sweden

Corresponding author: Remun Koirala (e-mail: remun.koirala@cea.fr).

This work was supported, in part, by the European H2020 project 5GCAR (GA No. 761510), the VINNOVA COPPLAR project, funded under Strategic Vehicle Research and Innovation Grant (GA No. 2015-04849), and the European H2020 project SECREDAS, which is funded through the specific ECSEL Joint Undertaking research and innovation program (GA No. 783119).

ABSTRACT In this paper, we propose various localization error optimal beamforming strategies and subsequently study the trade-off between data and localization services while budgeting time and frequency resources in a multi-user millimeter-wave framework. Allocating more resources for the data service phase instead of localization would imply higher data rate but, concurrently, also a higher position and orientation estimation error. In order to characterize this trade-off, we firstly derive a flexible application-dependent localization error cost function combining the Cramér-Rao lower bounds of delay, angle of departure and/or angle of arrival estimates at a mobile receiver over the downlink. Consequently we devise different fairness criteria based localization error optimal beamforming strategies in a multi-user context. Finally, we show the advantage of the latter beamforming strategies and assess the communication-localization trade-off with respect to various time-frequency resource division schemes.

INDEX TERMS Beam steering, Cramér-Rao Bounds, Localization, Millimeter wave communication, MIMO.

I. INTRODUCTION

An exponential increase in the demand for low latency high data rate services is driving the wireless communication industry into adopting high frequency millimeter wave (mm-Wave) as a key technology in the 5th generation (5G) of cellular networks [1]. These high frequency bands (between 30 and 300 GHz) are beneficial by allowing high data rates through the exploitation of large available bandwidths [2]. However, operating in the mm-Wave domain, as verified by Friis' transmission equation, is also characterized by high path loss, high shadowing loss and high sensitivity to blockages [3]. To combat these issues, beamforming with the help of highly directional, steerable and compact antenna arrays is considered an effective solution to provide high directivity gain and hence, improve the signal-to-noise ratio (SNR) [4], [5].

However, effective beamforming calls for even better knowledge of the propagation channel than within omni-

directional transmissions. In the literature, mm-Wave channel estimation is usually split into two phases: i) Beam training, typically based on spatial beam sweeping [6], [7] and ii) Channel parameters estimation (in both single- and multi-path scenarios), relying for instance on optimization and compressive sensing techniques [8]–[10]. The objective of the latter is to exploit the sparse geometric structure of the mm-Wave channel to estimate the angle of departure (AoD), the angle of arrival (AoA) and the complex channel coefficients of a few well-separated multi-path components. In the mm-Wave case, knowing the position and orientation of the user and beyond, knowing the relative geometry of a given radio link (e.g., by means of AoD and AoA estimates), is highly beneficial, for instance for faster initial access, eased beam alignment, dynamic user tracking, *etc* [11], [12].

Initial works on mm-Wave localization aimed at characterizing the performance bounds of location-dependent variables estimation, mostly in terms of their Cramér-Rao lower

bound (CRLB). In [9], [13]–[15] for instance, the authors derive the CRLB of delay, AoD and AoA estimation for single-carrier systems in both single- and multi-path scenarios. In [15], the authors derive a similar CRLB formulation in a multi-path scenario, while making strong asymptotic assumptions regarding the occupied bandwidth and the number of transmit and receive antenna elements. In [14], a comparison between Multiple Input Multiple Output (MIMO) and beamforming architectures is provided, showing that the effect of multi-path can be neglected when assuming massive antenna arrays. In [9] the authors characterize the CRLB for the same location-dependent estimation variables, but within multi-carrier systems. Using these theoretical performance bounds, recent works in the literature have also been dedicated towards finding the localization optimal beamformers. In particular, [16] and [17] study localization bounds based beamforming in a single-user context with both single and multiple subcarriers. Similarly, in [18], the authors propose beamforming strategies to minimize a localization error expressed in the form of the squared position error bound (SPEB). This SPEB is shown to be equivalent to a linear combination of the CRLB terms associated with delay and AoD estimates. Furthermore, [19] studies different fairness policies for localization error optimal beamforming in a multi-user multi-carrier system.

Beyond, aiming at drawing inherent synergies and mutual benefits between the two functionalities, the simultaneous localization and communication framework (also referred to as multi-service) has also been gaining popularity in this specific context of mm-Wave. For instance, Destino *et al.* [20], [21] explore the trade-off between position estimation error bounds (PEB) and/or orientation estimation error bounds (OEB) on the one hand, and communication data rates on the other hand, as a result of time sharing between the two services for both single- and multi-user cases. Similarly, in [22], the authors investigate different beam training strategies and the corresponding trade-offs between communication and positioning. Likewise, the authors study optimal beamwidth selection with energy [19] and power [23] budgeting schemes between localization and communication services in a single-user scenario.

In this paper, we study different resource budgeting strategies in a framework consisting of both communication and localization services¹ for multi-user cases in a multi-carrier system. For this purpose, we first derive the localization optimal beamformers and then recall the communication oriented optimal beamformers for both single and multiple users from [21]. For the localization oriented optimal beamformer, we then reformulate the CRLB characterizing the estimation of key channel parameters such as delay, AoD, AoA and the complex channel coefficient in a multi-carrier scenario. Based on the previous bounds, we subsequently construct a tunable localization error cost function combining the latter

¹Here, we consider communication and localization as two independent services, unlike in a joint localization and communication scenario, where the output of one service is fed back into the input of another.

intermediary bounds, before formulating and solving out the beamforming optimization problem accordingly.

In comparison with the existing works reported above, the main paper contributions can be summarized as follows.

- 1) Reformulation of the Fisher Information Matrix (FIM) for the joint estimation of all the previously mentioned channel parameters in a multi-carrier case and consequently, derivation of the CRLB in terms of delay, AoD and AoA.
- 2) With the help of the previous CRLB, derivation of the localization error as a properly weighted function of squared PEB and OEB. Reformulation of the function into a flexible and tunable localization error cost function, enabling to put the strength onto intermediary location-dependent estimated variables, depending on the underlying application.
- 3) Optimal beamforming optimization problem considering the formulated localization error for both single- and multi-user cases, further convex reformulation of the previous optimization problem and proposal of an adapted solution accordingly. In the multi-user scenario, formulation of a beam gain sharing strategy based on two distinct fairness criteria, namely proportional and min-max fairness.
- 4) Illustration and investigation of the system-level communication and localization trade-off for different resource sharing strategies (in particular time and frequency) for multi-user scenarios and comparison of these strategies, given a certain resource budget.

The rest of the paper is organized as follows. In section II we introduce our system model. In section III we present the FIM and CRLB derivation for a single- and multi-carrier cases. We formulate the localization error, before introducing and solving the localization based optimization problem in section IV. Similarly, we also recall the data rate optimal beamforming solution from state of the art. In section V, we present possible localization and communication frameworks in terms of frequency and time budgeting and the trade-off that arises from the different presented strategies. We provide and discuss various illustrations of optimized beamforming results in a canonical scenario in section VI. We also extensively compare the resource allocation schemes by means of Monte Carlo simulations, providing insights in terms of system design. Finally, the paper concludes in section VII.

II. SYSTEM MODEL

Consider a wireless mm-Wave down-link scenario consisting of a base station (BS) equipped with N_t antenna elements and U users, each equipped with N_r antenna elements. The positions of the BS and user- u are represented by $\mathbf{p} = [p_x, p_y]^T \in \mathbb{R}^2$ and $\mathbf{q}_u = [q_{x,u}, q_{y,u}]^T \in \mathbb{R}^2$ respectively. Similarly, the orientation of user- u , relative to the y -axis as illustrated in Fig. 1, is given by $\mathbf{o}_u \in [0, 2\pi)$. In our system, we consider that the BS has coarse knowledge of the user position and orientation.

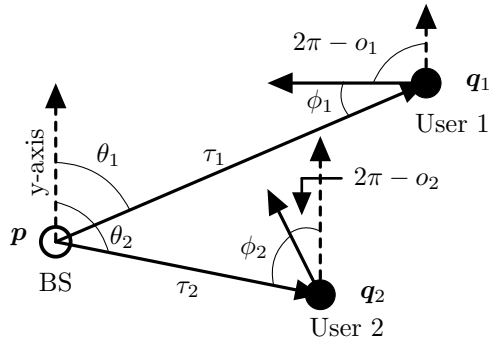


FIGURE 1. Example of deployment with 1 BS and 2 users with orientations o_1 and o_2 at locations q_1 and q_2 respectively

The complex signal at a generic time instant is transmitted across N subcarriers centered around frequency f_c with bandwidth B and duration T_s and is referred to as s_n for the n -th subcarrier where $n \in \{-\frac{N}{2}, \dots, \frac{N}{2}\}$. We denote the i -th element of the previous set at n_i where $i = 1, 2, \dots, N$.

Let $\mathbf{f}_n \in \mathbb{C}^{N_t}$ denote the beamformer in the precoding sense for the n -th subcarrier. We consider limited beamforming power $0 \leq \text{trace}(\mathbf{f}_n \mathbf{f}_n^H) \leq 1$ to satisfy the spectral mask set by regulations. In this paper, we consider uniquely the direct path, assuming a line-of-sight (LOS) propagation model [13], [18]. The $N_r \times N_t$ complex channel matrix for the n -th subcarrier between the BS and user- u is denoted by $\mathbf{H}_{u,n}$ and formulated as in [6].

$$\mathbf{H}_{u,n} = \sqrt{\xi_u} h_u e^{-j2\pi\tau_u \frac{nB}{N}} \mathbf{a}_{\text{Rx},u}(\phi_u) \mathbf{a}_{\text{Tx},u}^H(\theta_u), \quad (1)$$

where $h_u \in \mathbb{C}$ is the complex channel coefficient, ξ_u is the path-loss between the BS and the user, and τ_u , θ_u and ϕ_u are the delay, AoD and AoA respectively associated with user u . Both the transmitting and receiving antenna arrays are assumed to be uniform linear array (ULA). Assuming an odd number of antenna elements and the centroid of the array as the reference point, the antenna array response can be expressed as

$$\mathbf{a}_{\text{Tx},u} = \frac{1}{\sqrt{N_t}} \left[e^{-j(\frac{N_t+1}{2}-1)\frac{2\pi}{\lambda_c} d \cos(\theta_u)}, \dots, 1, \dots, e^{-j(\frac{N_t+1}{2}-N_t)\frac{2\pi}{\lambda_c} d \cos(\theta_u)} \right]^T. \quad (2)$$

where, λ_c is the wavelength corresponding to the center frequency of the transmitted signal and d is the inter-element distance. For the ease of notation, we write $\mathbf{a}_{\text{Tx},u}(\theta_u)$ as $\mathbf{a}_{\text{Tx},u}$ and do the same for $\mathbf{a}_{\text{Rx},u}(\phi_u)$. Likewise, $\mathbf{a}_{\text{Rx}}(\phi_u)$ can be expressed by simply replacing θ_u by ϕ_u and N_t by N_r in equation (2). We assume no beam squinting effects, hence the antenna array responses are independent of subcarrier frequencies.

We consider the received signal $y_{u,n} \in \mathbb{C}$ at the user- u after whitening and combining expressed as

$$y_{u,n} = \sqrt{P_{\text{Tx},u}} \mathbf{w}_u^H \mathbf{H}_{u,n} \mathbf{f}_n s_n + \tilde{n}_n, \quad (3)$$

where, $P_{\text{Tx},u}$ is the transmitted power with respect to the user and $\tilde{n}_n \in \mathbb{C}$ is the zero-mean additive white Gaussian noise (AWGN) with two-sided spectral density $N_0/2$ and $\mathbf{w}_u \in \mathbb{C}^{N_r}$ is the combiner vector at the mobile user.

III. FIM AND CRLB

Here, we will derive the FIM, firstly for the n -th subcarrier and then generalize it for all the subcarriers. Subsequently, we will derive the CRLB for joint delay, AoD and AoA estimation.

A. FIM IN THE SINGLE-CARRIER CASE

We define a set of parameters $\boldsymbol{\eta}_u = [\tau_u, \theta_u, \phi_u, h_{R,u}, h_{I,u}]$ comprising the estimation variables where $h_{R,u}$ and $h_{I,u}$ respectively represent the real and imaginary parts of the complex the channel coefficient. Then, the FIM $\mathbf{J}_{n,u} \in \mathbb{R}^{5 \times 5}$ characterizing the estimation of these parameters has been derived in [9], [13], [14], [16] as

$$\mathbf{J}_{u,n} = \begin{bmatrix} \Phi_n(\tau_u, \tau_u) & \Phi_n(\tau_u, \theta_u) & \Phi_n(\tau_u, \phi_u) & \Phi_n(\tau_u, h_{R,u}) & \Phi_n(\tau_u, h_{I,u}) \\ \Phi_n(\theta_u, \tau_u) & \Phi_n(\theta_u, \theta_u) & \Phi_n(\theta_u, \phi_u) & \Phi_n(\theta_u, h_{R,u}) & \Phi_n(\theta_u, h_{I,u}) \\ \Phi_n(\phi_u, \tau_u) & \Phi_n(\phi_u, \theta_u) & \Phi_n(\phi_u, \phi_u) & \Phi_n(\phi_u, h_{R,u}) & \Phi_n(\phi_u, h_{I,u}) \\ \Phi_n(h_{R,u}, \tau_u) & \Phi_n(h_{R,u}, \theta_u) & \Phi_n(h_{R,u}, \phi_u) & \Phi_n(h_{R,u}, h_{R,u}) & \Phi_n(h_{R,u}, h_{I,u}) \\ \Phi_n(h_{I,u}, \tau_u) & \Phi_n(h_{I,u}, \theta_u) & \Phi_n(h_{I,u}, \phi_u) & \Phi_n(h_{I,u}, h_{R,u}) & \Phi_n(h_{I,u}, h_{I,u}) \end{bmatrix}, \quad (4)$$

where the values of the matrix entries are given in Appendix A.

B. FIM IN THE MULTI-CARRIER CASE

The FIM for the multi-carrier case can be extended from equation (4) as [9]:

$$\mathbf{J}_u = \sum_{n=-N/2}^{N/2} \mathbf{J}_{u,n}. \quad (5)$$

Considering a symmetric power density of the transmitted signal (with respect to the central frequency) after beamforming by assuming $\mathbf{f}_{-n} = \mathbf{f}_n$ and $s_{-n} = s_n$, we can reformulate the FIM in a simple form as presented in Appendix B. By considering these assumptions, we significantly reduce the complexity of inverting the matrix for the derivation of CRLB, although we reduce the transmit diversity by a factor 2.

C. CRLB FORMULATION IN THE MULTI-CARRIER CASE

The symmetry assumption in the transmitted signal decouples the delay estimation with the rest of estimation variables in the FIM in equation (5), and hence, we can simply invert the delay Fisher information to get the CRLB for delay

estimation. For the AoD and AoA, we can use Schur's complement similar to [16] and find the CRLBs, as follows.

$$\Phi^{-1}(\tau_u, \tau_u) = \frac{\alpha_{\tau,u}}{\mathbf{a}_{\text{Tx},u}^H \mathbf{X} \tau \mathbf{a}_{\text{Tx},u}}, \quad (6a)$$

$$\Phi^{-1}(\theta_u, \theta_u) = \frac{\alpha_{\theta,u}}{\left(\hat{\mathbf{a}}_{\text{Tx},u}^H \mathbf{X} \hat{\mathbf{a}}_{\text{Tx},u} - \frac{|\hat{\mathbf{a}}_{\text{Tx},u}^H \mathbf{X} \mathbf{a}_{\text{Tx},u}|^2}{\mathbf{a}_{\text{Tx},u}^H \mathbf{X} \mathbf{a}_{\text{Tx},u}} \right)}, \quad (6b)$$

$$\Phi^{-1}(\phi_u, \phi_u) = \frac{\alpha_{\phi,u}}{\mathbf{a}_{\text{Tx},u}^H \mathbf{X} \mathbf{a}_{\text{Tx},u}}. \quad (6c)$$

where, the parameters $\alpha_{\tau,u} = (4\pi^2 \sigma_u d_{0,u} |h_u|^2)^{-1}$, $\alpha_{\theta,u} = (d_{0,u} \sigma_u |h_u|^2)^{-1}$, $\alpha_{\phi,u} = \left(\sigma_u |h_u|^2 \left(d_{2,u} - \frac{d_{1,u}^2}{d_{0,u}} \right) \right)^{-1}$ and $\hat{\mathbf{a}}_{\text{Tx},u}$, σ_u and $d_{i,u}$ for $i \in \{0, 1, 2\}$ are the intermediary variables fully defined in appendices A and B. We also define the beamformer dependent variables $\mathbf{X}_\tau = \sum_{n=-N/2}^{N/2} |s_n|^2 n^2 \mathbf{F}_n$, $\mathbf{X} = \sum_{n=-N/2}^{N/2} |s_n|^2 \mathbf{F}_n$ and $\mathbf{F}_n = \mathbf{f}_n \mathbf{f}_n^H$.

D. PEB AND OEB

In order to characterize the localization error bounds, we use PEB and OEB as measures of the localization accuracy as they are widely used in the literature [9], [16], [20]. Hence, in this section we introduce PEB and OEB which we can derive from the FIM in equation (5).

Consider $\boldsymbol{\mu}_u = [p_{x,u}, p_{y,u}, \alpha_u, h_{r,u}, h_{i,u}]$ be the vector comprising the new estimation variables representing user u 's 2D absolute Cartesian coordinates and absolute orientation, with the real and imaginary channel coefficients respectively. As derived in [9] and [20], the FIM in terms of the new parameters can be written as

$$\mathbf{J}_{\boldsymbol{\mu},u} = \mathbf{T}_u \mathbf{J}_u(\mathbf{X}_N) \mathbf{T}_u^T, \quad (7)$$

where \mathbf{T}_u is the Jacobian of $\boldsymbol{\mu}_u$ with respect to the original estimation variables in $\boldsymbol{\mu}_u$ formulated in equation (47).

Hence, we define PEB and OEB for user u as follows.

$$\text{PEB}_u = \sqrt{\text{trace}(\mathbf{J}_{\boldsymbol{\mu},u,1:2,1:2}^{-1}(\mathbf{X}_N))}. \quad (8)$$

$$\text{OEB}_u = \sqrt{\mathbf{J}_{\boldsymbol{\mu},u,3,3}^{-1}(\mathbf{X}_N)}. \quad (9)$$

IV. POSITIONING ERROR AND DATA RATE FORMULATION IN THE SINGLE- AND MULTI-USER CASES

Our main goal is to study the trade-off between data rate and localization considering various transmission strategies. For this sake, we have to find the optimal beamformer with respect to both the localization and data rate services. In this section, we will first formulate the equivalent localization error as the sum of squared PEB and OEB and then formulate the beamforming optimization problem accordingly. Then we will address the data service part by simply recalling the conventional communication oriented optimal beamformer.

A. POSITIONING ERROR IN THE SINGLE-USER CASE

We characterize an equivalent overall localization error resulting from the combined squared PEB and OEB. As we can see in the derivation in Appendix C, the localization error can be formulated as a weighted linear combination of corresponding unitary CRLBs of the three location-dependent variables.

$$L_u(\mathbf{X}, \mathbf{X}_\tau) = \beta_\tau \Phi^{-1}(\tau_u, \tau_u) + \beta_\theta \Phi^{-1}(\theta_u, \theta_u) + \beta_\phi \Phi^{-1}(\phi_u, \phi_u), \quad (10)$$

Here, in order to have a generic optimization framework, we replace the weights with the tunable parameters² β_τ , β_θ , $\beta_\phi \geq 0$ for each estimation variable, namely delay, AoD, AoA respectively. The goal is to find the beamformer that minimizes this localization error cost. With the generalized localization error formulation in equation (10), we can analyze the effect of each estimation parameter independently onto beamforming by adjusting the weights, which can depend on a priori application requirements.

We can however notice that there are two different variables \mathbf{X} and \mathbf{X}_τ in the formulation of the localization error, in equation (10). In order to maintain one unique optimization variable in the equation, we can restructure the latter as follows.

Let $M = N_t \times N$. Using the Kronecker product, we define vectors $\mathbf{a}_u = \mathbf{s} \otimes \mathbf{a}_{\text{Tx},u}$, $\hat{\mathbf{a}}_u = \mathbf{s} \otimes \hat{\mathbf{a}}_{\text{Tx},u}$ and $\mathbf{a}_{N,u} = \mathbf{s}_N \otimes \mathbf{a}_{\text{Tx},u}$, where $\mathbf{s} = [|s_{n_1}| \ |s_{n_2}| \ \dots \ |s_{n_N}|]^T$, $\mathbf{s}_N = [n_1^2 |s_{n_1}| \ n_2^2 |s_{n_2}| \ \dots \ n_N^2 |s_{n_N}|]^T$ and $\mathbf{X}_N \in \mathbb{C}^{M \times M}$ is defined as the block diagonal matrix consisting of the matrix \mathbf{F}_n over each subcarrier, expressed as

$$\mathbf{X}_N = \begin{bmatrix} \mathbf{F}_{n_1} & & & \\ & \mathbf{F}_{n_2} & & \\ & & \ddots & \\ & & & \mathbf{F}_{n_N} \end{bmatrix}. \quad (11)$$

Hence, the localization error can be reformulated as

$$L_u(\mathbf{X}_N) = \frac{\beta_\tau \alpha_{\tau,u}}{\mathbf{a}_{N,u}^H \mathbf{X}_N \mathbf{a}_{N,u}} + \frac{\beta_\theta \alpha_{\theta,u}}{\left(\hat{\mathbf{a}}_u^H \mathbf{X}_N \hat{\mathbf{a}}_u - \frac{|\hat{\mathbf{a}}_u^H \mathbf{X}_N \mathbf{a}_u|^2}{\mathbf{a}_u^H \mathbf{X}_N \mathbf{a}_u} \right)} + \frac{\beta_\phi \alpha_{\phi,u}}{\mathbf{a}_u^H \mathbf{X}_N \mathbf{a}_u}. \quad (12)$$

²With the new parameters, the localization error formulated in Appendix C becomes a special case of the formulation in equation (10) when $\beta_\tau = k_{\tau,u}$, $\beta_\theta = k_{\theta,u}$ and $\beta_\phi = k_{\phi,u}$. It must also be noted that the CRLB of the estimation variables are interrelated, as explained in [16]. It is inevitable that if we estimate a variable, we can estimate another one as well. The weights do not define the exclusivity of estimation of particular parameters, but rather the estimation variable on which the focus is. A motivation behind the introduction of the general cost function in equation (10) is that some applications might be more sensitive to angle or ranging errors than the absolute position error. In such cases, one can play with the weights β to tune the cost function depending on application requirements.

The goal now is to state an optimization problem which minimizes the localization error under a power constraint. This problem can be formulated as:

$$\min_{\mathbf{X}_N} L_u(\mathbf{X}_N), \quad (13a)$$

subject to:

$$\text{trace}(\mathcal{I}_i^T \mathbf{X}_N \mathcal{I}_i) \leq 1, \quad \forall i, \quad (13b)$$

$$\text{trace}(\mathcal{I}_i^T \mathbf{X}_N \mathcal{I}_i) \geq 0, \quad \forall i, \quad (13c)$$

$$\mathcal{I}_i^T \mathbf{X}_N \mathcal{I}_j = \mathbf{0}_{N_t}, \quad \forall i, j : i \neq j, \quad (13d)$$

$$\text{trace}(\mathbf{X}_N) = K, \quad (13e)$$

$$\mathbf{X}_N \succeq 0, \quad (13f)$$

$$\text{rank}(\mathcal{I}_i^T \mathbf{X}_N \mathcal{I}_i) = 1 \quad \forall i. \quad (13g)$$

where $i, j \in \{1, 2, \dots, N\}$, $\mathbf{0}_{N_t} \in \mathbb{R}^{N_t \times N_t}$ represents the zero matrix sized $N_t \times N_t$ and $\mathcal{I}_n \in \mathbb{R}^{N_t \times M}$ represents a matrix consisting of identity matrix \mathbf{I}_{N_t} of size $N_t \times N_t$ in n -th block position and $\mathbf{0}_{N_t}$ in the rest of the block positions; in other words,

$$\mathcal{I}_n = \mathbf{e}_n \otimes \mathbf{I}_{N_t} \quad (14)$$

where $\mathbf{e}_n \in \mathbb{R}^{N \times 1}$ is the N -dimensional Euclidean space standard basis vector whose values are all 0s except the n -th element, which is equal to 1.

The constraints from equations (13b) and (13c) define the power constraint at each subcarrier as assumed in the system model. Likewise, equation (13d) enforces the block diagonality constraint in the matrix \mathbf{X}_N . Equation (13e) represents the total power constraint across all the subcarriers and by the virtue of equation (13b), we know that $K \leq N$. Similarly, from the positive semidefinite structure of the individual blocks \mathbf{F}_n in \mathbf{X}_N , we can conclude that \mathbf{X}_N is positive semidefinite as well and the rank of each block is 1.

The objective function along with some constraints in this equation, however, are non convex. However, it is possible to reformulate it into a convex optimization problem by introducing different slack variables $\zeta_\tau, \zeta_\theta, \zeta_\phi$ and represent the problem as follows:

$$\max_{\mathbf{X}_N, \zeta_\theta, \zeta_\phi, \zeta_\tau} \beta_\theta \zeta_\theta + \beta_\phi \zeta_\phi + \beta_\tau \zeta_\tau, \quad (15a)$$

subject to:

$$\frac{\mathbf{a}_{N,u}^H \mathbf{X}_N \mathbf{a}_{N,u}}{\alpha_{\tau,u}} \geq \zeta_\tau, \quad (15b)$$

$$\frac{1}{\alpha_{\theta,u}} \left(\mathbf{a}_u^H \mathbf{X}_N \mathbf{a}_u - \frac{|\mathbf{a}_u^H \mathbf{X}_N \mathbf{a}_u|^2}{\mathbf{a}_u^H \mathbf{X}_N \mathbf{a}_u} \right) \geq \zeta_\theta, \quad (15c)$$

$$\frac{\mathbf{a}_u^H \mathbf{X}_N \mathbf{a}_u}{\alpha_{\phi,u}} \geq \zeta_\phi, \quad (15d)$$

$$(13b)-(13g).$$

Note that the constraints from equations (15b) and (15d) are affine. From [24] and Appendix D, we can simplify and cast

the hyperbolic constraint in equation (15c) as

$$\left\| \begin{bmatrix} 2\Re(\mathbf{a}_u^H \mathbf{X}_N \mathbf{a}_u) \\ 2\Im(\mathbf{a}_u^H \mathbf{X}_N \mathbf{a}_u) \\ \mathbf{a}_u^H \mathbf{X}_N \mathbf{a}_u - \zeta_\theta \alpha_{\theta,u} - \mathbf{a}_u^H \mathbf{X}_N \mathbf{a}_u \end{bmatrix} \right\|_2 \leq \mathbf{a}_u^H \mathbf{X}_N \mathbf{a}_u - \zeta_\theta \alpha_{\theta,u} + \mathbf{a}_u^H \mathbf{X}_N \mathbf{a}_u. \quad (16)$$

where $\Re(\cdot)$ and $\Im(\cdot)$ represents the real and imaginary operators.

The objective function and all the constraints in equation (15), except the rank constraint in equation (13g), are convex. In order to solve this problem, in the literature, it is common to solve first a (sub-)problem after dropping the incriminated constraint. Then, based on the first step optimization result, one gets the best rank-1 approximation for the matrix of interest. The rank-1 approximation of the matrix \mathbf{F}_n^* as in [25] is given by

$$\mathbf{f}_n^* = \sqrt{\lambda_n} \mathbf{v}_n, \quad (17)$$

where λ_n is the largest eigenvalue of each block element \mathbf{F}_n^* of \mathbf{X}_N^* and \mathbf{v}_n is the corresponding eigenvector. Hence, replacing the constraint in equation (15c) with equation (16) and removing the rank constraint, we can easily solve the convex semidefinite problem with efficient solvers [26].

B. POSITIONING ERROR IN THE MULTI-USER CASE

Similarly, for a multi-user case, we define the overall localization error as a function of the localization error per user.

$$L(\mathbf{X}_N) = f(L_1(\mathbf{X}_N), L_2(\mathbf{X}_N), \dots, L_U(\mathbf{X}_N)). \quad (18)$$

For this multi-user scenario, we consider fairness criteria based beamforming strategies according to which we define the function $f(\cdot)$. The idea is to allocate power to different users based on their positions with the help of beamforming optimization in order to minimize the localization error.

1) Min Max Fairness Strategy

In this strategy, we ensure a minimum localization error requirement for each user. In doing so, we are limited by the worst user, hence the optimal solution would lead to the minimization of the localization error of the user with the maximum error. In this case, the objective function $L(\mathbf{X}_N)$ would be $\max(L_1(\mathbf{X}_N), L_2(\mathbf{X}_N), \dots, L_U(\mathbf{X}_N))$.

The optimization problem is thus formulated accordingly,

as follows:

$$\max_{\mathbf{X}_N, \zeta_\theta, \zeta_\phi, \zeta_\tau} \beta_\theta \zeta_\theta + \beta_\phi \zeta_\phi + \beta_\tau \zeta_\tau \quad (19a)$$

subject to:

$$\frac{\mathbf{a}_{N,u}^H \mathbf{X}_N \mathbf{a}_{N,u}}{\alpha_{\tau,u}} \geq \zeta_\tau, \quad \forall u \quad (19b)$$

$$\left\| \begin{bmatrix} 2\Re(\dot{\mathbf{a}}_u^H \mathbf{X}_N \mathbf{a}_u) \\ 2\Im(\dot{\mathbf{a}}_u^H \mathbf{X}_N \mathbf{a}_u) \\ \dot{\mathbf{a}}_u^H \mathbf{X}_N \dot{\mathbf{a}}_u - \zeta_\theta \alpha_{\theta,u} - \mathbf{a}_u^H \mathbf{X}_N \mathbf{a}_u \end{bmatrix} \right\|_2 \leq \dot{\mathbf{a}}_u^H \mathbf{X}_N \dot{\mathbf{a}}_u - \zeta_\theta \alpha_{\theta,u} + \mathbf{a}_u^H \mathbf{X}_N \mathbf{a}_u, \quad \forall u \quad (19c)$$

$$\frac{\mathbf{a}_u^H \mathbf{X}_N \mathbf{a}_u}{\alpha_{\phi,u}} \geq \zeta_\phi, \quad \forall u \quad (19d)$$

(13b)-(13g)

Note that the constraints in (19b)-(19d) have the same CRLB requirement for each of the estimation parameters (ζ_τ , ζ_θ and ζ_ϕ) for each user. This condition serves to maximize the performance of the worst user.

2) Proportional Fairness Strategy

Alternatively, we can have a proportionally fair beamforming where better users receive proportionally more power and hence have lower localization errors compared to worse users. We use sum log as the function $f(\cdot)$ in equation (18) and then have separate CRLB requirements for each user in order to achieve this proportionality while distributing the power. It has been shown that the diminishing return property of the log function can be used to achieve proportional fairness [27]. The objective function, in this case, would be $\sum_{u=1}^U \log(L_u(\mathbf{X}_N))$

The optimization problem can be written as

$$\max_{\mathbf{X}_N, \zeta_\theta, \zeta_\phi, \zeta_\tau, u} \sum_{u=1}^U \log(\beta_\theta \zeta_{u,\theta} + \beta_\phi \zeta_{u,\phi} + \beta_\tau \zeta_{u,\tau}) \quad (20a)$$

subject to:

$$\frac{\mathbf{a}_{n,u}^H \mathbf{X}_N \mathbf{a}_{n,u}}{\alpha_{\tau,u}} \geq \zeta_{\tau,u}, \quad \forall u \quad (20b)$$

$$\left\| \begin{bmatrix} 2\Re(\dot{\mathbf{a}}_u^H \mathbf{X}_N \mathbf{a}_u) \\ 2\Im(\dot{\mathbf{a}}_u^H \mathbf{X}_N \mathbf{a}_u) \\ \dot{\mathbf{a}}_u^H \mathbf{X}_N \dot{\mathbf{a}}_u - \zeta_{\theta,u} \alpha_{\theta,u} - \mathbf{a}_u^H \mathbf{X}_N \mathbf{a}_u \end{bmatrix} \right\|_2 \leq \dot{\mathbf{a}}_u^H \mathbf{X}_N \dot{\mathbf{a}}_u - \zeta_{\theta,u} \alpha_{\theta,u} + \mathbf{a}_u^H \mathbf{X}_N \mathbf{a}_u, \quad \forall u \quad (20c)$$

$$\frac{\mathbf{a}_u^H \mathbf{X}_N \mathbf{a}_u}{\alpha_{\theta,u}} \geq \zeta_{\theta,u}, \quad \forall u \quad (20d)$$

(13b)-(13g)

Since we solved the optimization problems in equations (19) and (20) without the rank constraints to maintain convexity of the problem, we perform the rank-1 approximation of matrix \mathbf{F}_n^* as for the single-user case in equation (17).

We can see that objective function for min max fairness scheme in equation (19a) is a linear maximization problem with $N_t^2 N + 3$ variables whereas that for the proportional fairness scheme is a non linear optimization problem in equation (20a) with $N_t^2 N + 3U$ optimization variables. The number of constraints in both the cases are the same. Hence, we expect the complexity of solving both the problems to increase with increasing N_t, U and N . Similarly, we expect the complexity of solving the optimization problem for proportional fairness scheme to be higher than that of min max fairness scheme due to the non linearity and larger number of optimization variables.

C. DATA RATE IN THE SINGLE- AND MULTI-USER CASES

Following the beamforming optimization in the localization phase, in this section we look at a data rate optimal beamforming solution existing in the literature. In consistency with the localization phase, we consider using an analog architecture with 1 radio frequency (RF) chain³ transmitting one stream of data at a time.

We assume that the beamformer transmits sequentially to the users across time *i.e.* one user at a time. Hence, for user- u , from the signal model in equation (3), we can express SNR as:

$$\text{SNR}_u = \frac{1}{N_0} \sum_{n=n_1}^{n_N} P_{\text{Tx},u} |\mathbf{w}_u^H \mathbf{H}_{u,n} \mathbf{f}_{n,u}|^2 |s_n|^2, \quad (21a)$$

$$= \frac{1}{N_0} \sum_{n=n_1}^{n_N} P_{\text{Tx}} |s_n|^2 \xi_u |h_u|^2 |\mathbf{w}_u^H \mathbf{a}_{\text{Rx},u}|^2 \mathbf{a}_{\text{Tx},u}^H \mathbf{F}_{u,n} \mathbf{a}_{\text{Tx},u}, \quad (21b)$$

$$= \frac{1}{N_0} \mathbf{a}_{\zeta,u}^H \mathbf{X}_{N,u} \mathbf{a}_{\zeta,u}, \quad (21c)$$

where,

$$\mathbf{a}_{\zeta,u} = [\zeta_u |s_{n_1}| \mathbf{a}_{\text{Tx},u}^T \quad \cdots \quad \zeta_u |s_{n_N}| \mathbf{a}_{\text{Tx},u}^T]^T \in \mathbb{C}^M \quad (22)$$

, and $\zeta_u = \sqrt{P_{\text{Tx}}} \sqrt{\xi_u} |h_u| |\mathbf{w}_u^H \mathbf{a}_{\text{Rx},u}|$.

The sum rate for U users, can now be formulated as

$$R = \sum_{u=1}^U R_u = \sum_{u=1}^U \frac{T_u}{T_C} \log_2(1 + \text{SNR}_u), \quad (23a)$$

$$= \sum_{u=1}^U \frac{T_u}{T_C} \log_2 \left(1 + \frac{\mathbf{a}_{\zeta,u}^H \mathbf{X}_{N,u} \mathbf{a}_{\zeta,u}}{N_0} \right). \quad (23b)$$

where, T_u is the fraction of time allocated for data communication phase for a particular user. Mathematically

³Note that the primary focus of this work is on beamforming optimization for the localization phase. In this section we look at a simple example with analog beamforming architecture for the communication phase for the resource allocation trade-off study. However, the choice of a beamforming architecture and the optimal beamformer for communication can be independent as any type of solution can be implemented on top of our beamforming optimization framework.

$\sum_{u=1}^U T_u = T_C$. The optimization can then be formulated similarly to [21] as follows

$$(P) : \max_{\mathbf{X}_N, T_u} R \quad (24a)$$

subject to:

$$R_u \geq \kappa, \quad (24b)$$

$$\sum_{u=1}^U T_u = T_C, \quad (24c)$$

$$(13b)-(13g).$$

Since we consider beamforming with respect to one user at a time, we can separate the optimization problem (P) into two separate optimization problems (P1) and (P2), the first one concerning the optimal beamforming vector per user and the second concerning the allocation of time T_u depending on the minimum rate requirement constraint for the u -th user in the sum rate maximization. The first optimization problem (P1) can be formulated as:

$$(P1) : \max_{\mathbf{X}_{N,u}} \text{SNR}_u \quad (25a)$$

subject to:

$$(13b)-(13g).$$

The above optimization problem (P1) concerns the beamforming optimization in a given direction for a particular user. The solution to the problem is a well known problem in the literature [20], [28], [29] referred to as conventional beamforming (CBF) and expressed as follows

$$\mathbf{X}_{N,u}^* = \text{diag}(\mathbf{F}_u^*, \mathbf{F}_u^*, \dots, \mathbf{F}_u^*), \quad (26)$$

where, $\mathbf{F}_u^* = \mathbf{f}_u^* \mathbf{f}_u^{*H}$ and

$$\mathbf{f}_u^* = \frac{\mathbf{a}_{\zeta,u}}{\|\mathbf{a}_{\zeta,u}\|_2}. \quad (27)$$

Since the SNR expression does not depend on the subcarrier frequency, the optimal beamformer is the same across all the subcarriers.

Now given the optimal beamforming vector for each user, we need to determine how much fraction of time T_C should be allocated to each user. Accordingly, the second optimization problem can be written as:

$$(P2) : \max_{T_u} R \quad (28a)$$

subject to:

$$\mathbf{X}_{N,u} = \mathbf{X}_{N,u}^* \quad (28b)$$

$$(24b),(24c).$$

For the problem (P2), the solution would be to allocate time firstly to fulfill the minimum rate requirement per user from equation (24b), then to allocate all the remaining time to the user with the highest SNR_u in order to maximize the sum rate. Hence the optimal solution would be:

$$T_u^* = \frac{\kappa}{\log_2(1 + \text{SNR}_u)} T_C + z_u^*, \quad (29)$$

where,

$$z_u^* = \begin{cases} \delta T_C & \text{if } \text{SNR}_u = \max(\text{SNR}_1, \dots, \text{SNR}_U) \\ 0 & \text{otherwise} \end{cases} \quad (30)$$

where, $\delta = 1 - \sum_{u=1}^U \kappa / \log_2(1 + \text{SNR}_u)$.

V. TRADE-OFF BETWEEN LOCALIZATION AND COMMUNICATION SERVICES

In this section, we will define different resource allocation strategies addressing both communication and localization needs. After having determined both localization and communication optimal beamformers, we consider a system framework providing both localization and communication functionalities. We acknowledge that it is possible to utilize the native communication signal for positioning services. However, it can lead to sub-optimal localization performance (e.g. see [30] for a discussion on localization specific waveforms), and hence we use dedicated pilots designed for better localization performance. In such a framework, the idea is to investigate and compare several schemes enabling resource sharing in both single- and multi-user cases. For a fixed resource budget, based on the trade-off and Quality of Service (QoS) requirement for each service, we determine the optimal split between the resources. Let $\mathbf{X}_{L,u}^*$ and \mathbf{X}_L^* represent the single- and multi-user optimal localization beamformers \mathbf{X}_N from equations (15) and (19) or (20) respectively. Similarly, let $\mathbf{X}_{C,u}^*$ and T_u^* represent the data rate optimal beamformer and optimal time allocation per user from equations (26) and (28) respectively.

A. TIME DIVISION

Consider a system level framework with total time budget of $T = T_L + T_C$, where T_L is the total time budgeted for localization, and the rest of the time T_C is allocated for communication. We investigate the trade-off between localization and communication performances as a result of time sharing between the two services.

For the multi-user scenario, we use two different schemes, namely the simultaneous localization and communication framework and the sequential⁴ localization and communication framework. In the former, we simultaneously localize all the users in the first phase and then simultaneously communicate with them. In the latter, we perform localization and communication for the first user independently and then for the second independently and so on.

a: Simultaneous multi-user assessment

In this strategy, all the users are simultaneously localized for a complete localization time duration of T_L , even though allocating simultaneous localization pilots to different users

⁴Here, the words simultaneous and sequential shall be intended in terms of multi-user assessment (and not in terms of communication or localization functionalities). The word "simultaneous" refers to a scenario when all the users are assessed at once, and "sequential" refers to a scenario when the users are assessed one by one.

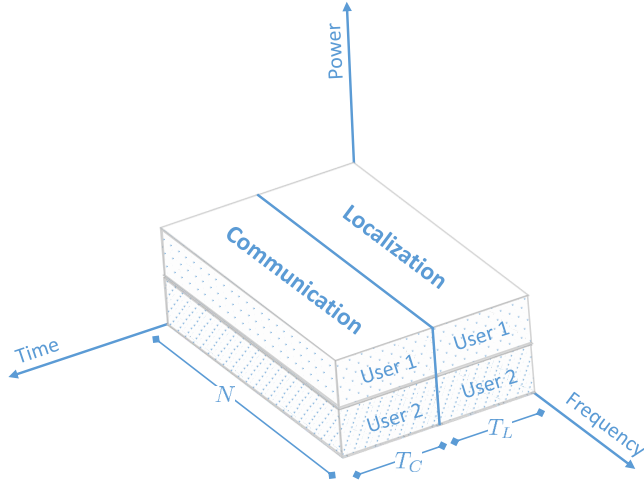


FIGURE 2. Time division in a localization and communication framework with simultaneous users assessment

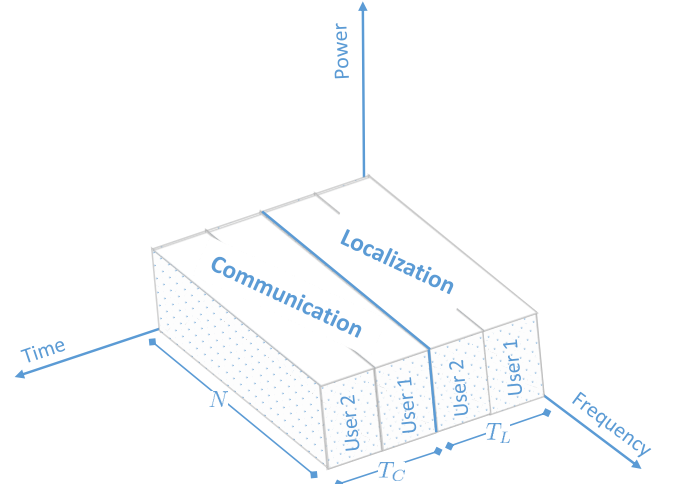


FIGURE 3. Time division in a localization and communication framework with sequential users assessment

means that each localization signal has reduced power as shown in Fig. 2. Likewise, we have the same situation for the communication phase in this scenario. In this case we use the optimal beamforming vector for multiple users \mathbf{X}_L^* and $\mathbf{X}_{C,u}^*$ for both localization and communication services respectively. We then look at the resulting average performance per user while considering data rate, PEB and OEB.

The average rate per user is

$$R = \frac{1}{U} \frac{T_C}{T} \sum_{u=1}^U \frac{T_u^*}{T_C} \log_2 \left(1 + \frac{\mathbf{a}_{\zeta,u}^H \mathbf{X}_{C,u}^* \mathbf{a}_{\zeta,u}}{N_0} \right). \quad (31)$$

Similarly, the average PEB and OEB per user with localization time limited to T_L can be written as⁵

$$\text{PEB} = \frac{1}{U} \sum_{u=1}^U \sqrt{\frac{T_s}{T_L} \text{trace} \left(\mathbf{J}_{\mu,u,1:2,1:2}^{-1}(\mathbf{X}_L^*) \right)}, \quad (32)$$

and,

$$\text{OEB} = \frac{1}{U} \sum_{u=1}^U \sqrt{\frac{T_s}{T_L} \mathbf{J}_{\mu,u,3,3}^{-1}(\mathbf{X}_L^*)}. \quad (33)$$

b: Sequential multi-user assessment

In this scheme, we localize and communicate with one single-user at a time, while assessing sequentially the multiple users. In this strategy, for localization and communication phases, at each time instance, one single-user is served with maximum power but only for a reduced time duration of T_L/U and T_u for localization and communication respectively as shown in Fig. 3, thus respecting the same overall constraints on time T_L and T_C as in the previous allocation

⁵The FIM in [17], [20] is considered for a signal with duration T_s . Since we consider a localization time of T_L , we consider the information increase by a factor of T_L/T_s (e.g., equivalently, performing a coherent integration of successive observations/estimates would reduce noise by the same factor).

scheme. In other words, we basically use the single-user time division strategy for U consecutive periods, once for each user.

The average rate per user can be written as equation (31).

Similarly, the average PEB and OEB per user with the localization time limited to T_L/U can be written as

$$\text{PEB} = \frac{1}{U} \sum_{u=1}^U \sqrt{\frac{UT_s}{T_L} \text{trace} \left(\mathbf{J}_{\mu,u,1:2,1:2}^{-1}(\mathbf{X}_{L,u}^*) \right)}, \quad (34)$$

and,

$$\text{OEB} = \frac{1}{U} \sum_{u=1}^U \sqrt{\frac{UT_s}{T_L} \mathbf{J}_{\mu,u,3,3}^{-1}(\mathbf{X}_{L,u}^*)}. \quad (35)$$

B. FREQUENCY DIVISION

In this strategy, we share the available subcarriers for both localization and communication simultaneously for the full duration of time T . Let \mathcal{N}_L and \mathcal{N}_C represent the sets of subcarriers dedicated for localization and communication respectively and $N_L = |\mathcal{N}_L|$ and $N_C = |\mathcal{N}_C|$ represent the cardinality of the two sets. We further need to split the subcarriers allocated to the communication phase into U parts, represented as $\mathcal{N}_{C,u}, \forall u$, such that we can beamform all the U users relying on different subcarriers. Since we consider no frequency effect on the rate, we can split the frequency among the users arbitrarily. The sets \mathcal{N}_L and \mathcal{N}_C are mutually exclusive and $\bigcup_{u=1}^U \mathcal{N}_{C,u} = \mathcal{N}_C$. Let us define matrices $\mathbf{Y}_L = \text{diag}(\mathbf{Y}_{L,1}, \mathbf{Y}_{L,2}, \dots, \mathbf{Y}_{L,N}) \in \mathbb{R}^{M \times M}$ and $\mathbf{Y}_{C,u} = \text{diag}(\mathbf{Y}_{C,u,1}, \mathbf{Y}_{C,u,2}, \dots, \mathbf{Y}_{C,u,N}) \in \mathbb{R}^{M \times M}$ where

$$\mathbf{Y}_{L,n} = \begin{cases} \mathbf{I}_{N_t}, & \text{if } n \in \mathcal{N}_L \\ \mathbf{0}_{N_t}, & \text{otherwise} \end{cases} \quad (36)$$

$$\mathbf{Y}_{C,u,n} = \begin{cases} \mathbf{I}_{N_t}, & \text{if } n \in \mathcal{N}_{C,u} \\ \mathbf{0}_{N_t}, & \text{otherwise} \end{cases} \quad (37)$$

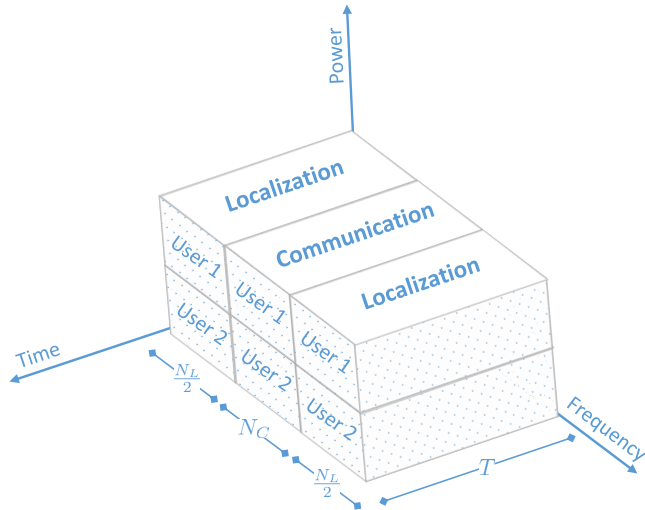


FIGURE 4. Frequency division framework for localization and communication services

Then, we can define the average data rate as

$$R = \frac{1}{U} \sum_{u=1}^U \log_2 \left(1 + \frac{\mathbf{a}_{\zeta,u}^H \mathbf{Y}_{C,u} \mathbf{X}_{C,u}^* \mathbf{Y}_{C,u}^T \mathbf{a}_{\zeta,u}}{N_0} \right). \quad (38)$$

Similarly, the average PEB and OEB per user for the multi-user case can be written as

$$\text{PEB} = \frac{1}{U} \sum_{u=1}^U \sqrt{\frac{T_s}{T} \text{trace}(\mathbf{J}_{\mu,u,1:2,1:2}^{-1}(\mathbf{Y}_L \mathbf{X}_L^* \mathbf{Y}_L^T))}, \quad (39)$$

and,

$$\text{OEB} = \frac{1}{U} \sum_{u=1}^U \sqrt{\frac{T_s}{T} \mathbf{J}_{\mu,u,3,3}^{-1}(\mathbf{Y}_L \mathbf{X}_L^* \mathbf{Y}_L^T)}. \quad (40)$$

The formulation $\mathbf{Y}_C \mathbf{X}_{C,u}^* \mathbf{Y}_C^T$ nullifies the beamformer related to the subcarriers not dedicated for communication (and likewise \mathbf{Y}_L for localization). Accordingly, the individual subcarriers, and thus the total power budgeted over the entire occupied bandwidth, can be split to cover the two different services.

VI. NUMERICAL RESULTS

In this section we provide some illustrations of optimized beamformers in a canonical multi-user scenario that can be seen in Fig. 5.

A. SYSTEM PARAMETERS AND SIMULATION SETUP

Let us consider a mm-Wave BS operating at $f_c = 38$ GHz with bandwidth $B = 300$ MHz. We fix the antenna elements number for both the BS and the user to $N_t = N_r = 30$ elements. We consider both the BS and the user antennas to have a gain of 13 dBi and an inter-element distance

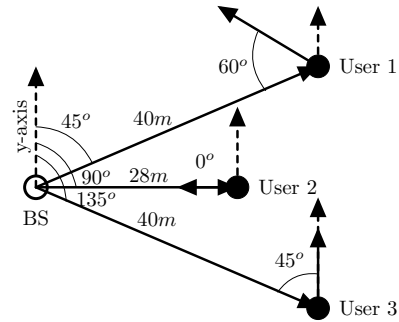


FIGURE 5. Example of canonical scenario with a BS and 3 users positioned at different distances from the BS with different orientation.

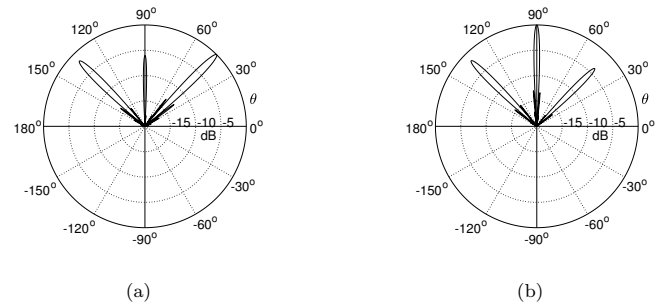


FIGURE 6. Example of normalized beam direction for a localization-optimized beamformer in the multi-user case, according to (a) min max and (b) proportional fairness strategies.

$d = 0.5\lambda_c$. The path loss ξ_u between the BS and any mobile user at a distance of d_u from the BS is given as in [31].

$$\xi_u(d_u)[\text{dB}] = \xi(d_0) + 10\alpha(d_u/d_0) + X_\sigma, \quad (41)$$

where, $\xi(d_0) = 10 \log_{10} (4\pi d_0 / \lambda_c)^2$ is the free space path loss for a reference distance $d_0 = 1m$. $\alpha = 1.9$ is the path loss exponent and $\sigma = 4.6$ dB is the standard deviation of the zero mean Gaussian random shadow factor X_σ respectively. We consider the illustrating canonical scenario shown in Fig. 5 as the system model, unless otherwise specified.

B. RESULTS AND ANALYSIS

In Fig. 6, we show the normalized beam gains as a function of BS transmission directions as a result of localization error optimal multi-user beamforming in the above canonical scenario. We observe variable levels of power transmitted in the directions of the three distinct users depending on the fairness strategy considered. From Fig. 5, we observe that User 2 is the best user due to its proximity and orientation towards the base station followed by User 3 which is at the same distance as User 1, but with a different orientation. This is evident in Fig. 6 as with the min max fairness strategy, User 1 is allocated relatively more power compared to with the proportional fairness strategy.

Using the same localization error optimal beamforming model, in Fig. 7 and 8 we can see the effect of β_τ on the subcarriers allocation. As discussed earlier, during localization, we consider symmetric power allocation across subcarriers

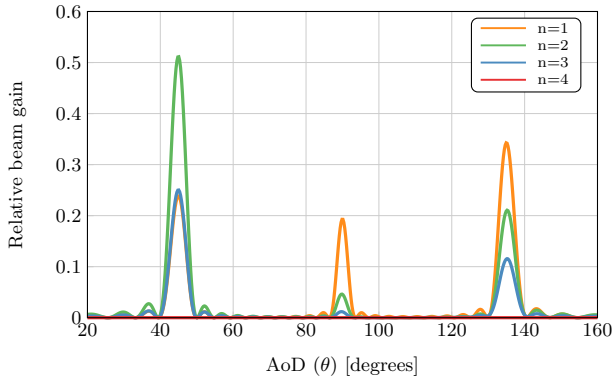


FIGURE 7. Example of normalized beam gain (with respect to total gain) with min max fairness strategy as a function of the direction in the multi-user case with $\beta_\tau = 1$, $\beta_\theta = 1$ and $\beta_\phi = 1$

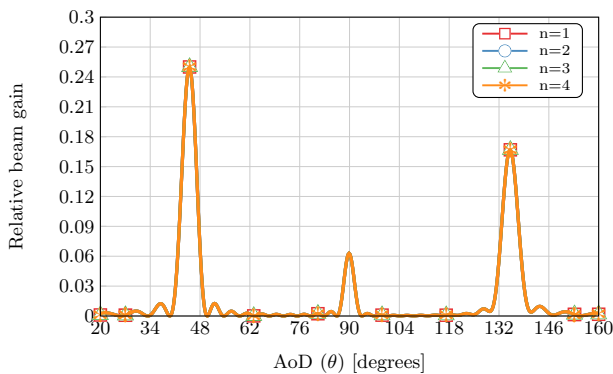


FIGURE 8. Example of normalized beam gain (with respect to total gain) with min max fairness strategy as a function of the direction in the multi-user case with $\beta_\tau = 0$, $\beta_\theta = 1$ and $\beta_\phi = 1$

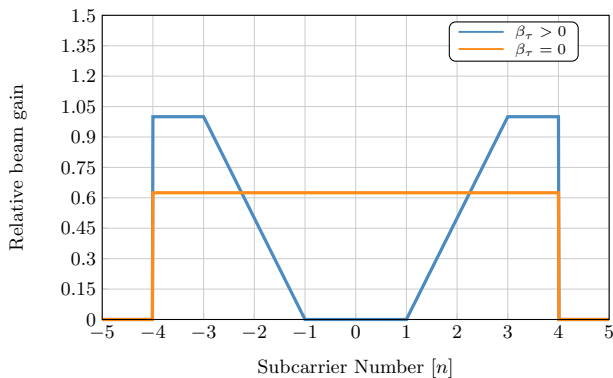


FIGURE 9. Power allocation per subcarrier for different values of β_τ

riers (with respect to the center frequency of the occupied spectrum) to facilitate the statement and resolution of the optimization problem we derived. Hence, to avoid repetition due to the underlying symmetry in our analysis, we only consider the repeated subcarriers. We consider 8 subcarriers in the full spectrum scenario, but only look at 4 of them numbered as $n = \{1, 2, 3, 4\}$. We limit the total power K to 2.5 units and optimize the beamformer with $\beta_\tau = 0$ or

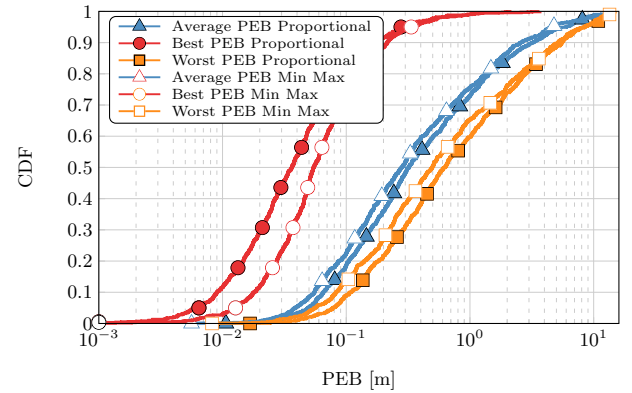


FIGURE 10. Empirical CDF of the PEB per user (best, worst and average performance) for different fairness strategies over 1000 MC trials.

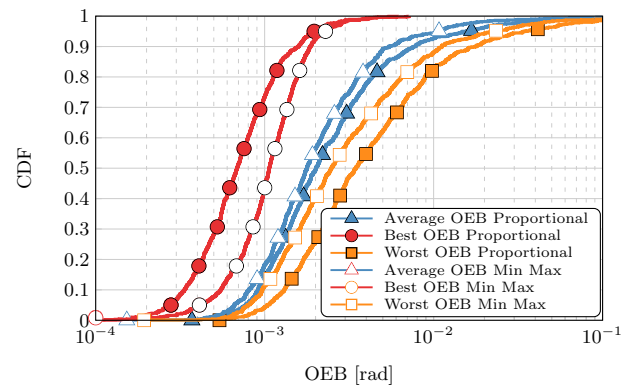


FIGURE 11. Empirical CDF of the OEB per user (best, worst and average performance) for different fairness strategies over 1000 MC trials.

$\beta_\tau > 0$. When $\beta_\tau > 0$, we can observe that in Fig. 7, the first subcarrier has no power allocated and the remaining subcarriers have unequal power distribution. However, for the other case where $\beta_\tau = 0$, we have equal allocation across all the subcarriers, as illustrated by Fig. 8. The subcarrier power distribution for the two cases are presented in Fig. 9. It is clear that for $\beta_\tau > 0$, the optimal beamformer would allocate all the power to the two extremities of the spectrum. The reason is that, for delay estimation, performance would benefit from higher resolution provided by a larger equivalent bandwidth (from using more distant frequency components). Hence in the figure, under the spectral power mask constraint (with $0 \leq \text{trace}(\mathbf{f}_n \mathbf{f}_n^H) \leq 1$), the optimal power allocation solution is vertical water-filling starting from the ends of the spectrum. In contrast, for AoD and AoA estimation, since the frequency plays no role according to the underlying model, there is a uniform power allocation over all the subcarriers.

Figs. 10 and 11 show the empirical cumulative distribution function (CDF) of best case, worst case and average PEB and OEB per user in the multi-user scenario, over 1000 Monte Carlo (MC) simulation trials of the user positions consisting of three random users positions/orientations (per trial) evaluated with both proportional and min max fairness strategies. In each occupied position of each MC trial, we use

the localization error optimal beamforming to characterize the best PEB as the one with minimum PEB, the worst PEB as the one with maximum PEB and the average PEB as the mean PEB over all three users (and similarly for OEB). We can observe that the CDFs of best, worst and average PEB and OEB are close to each other for all the cases. Even then, we can see that the proportional fairness, as expected, performs better for the best user whereas worse for the worst user and in average. It is also evident that the min max fairness improves the worst user performance, whereas the proportional fairness improves further the best user. Based on this observation, we can suggest that, if the dispersion is large between the worst and the best user, it is better to use the proportional fairness scheme such that the localization performance of the best user does not degrade too much whereas for a lower dispersion, min max optimization improves the overall performance more.

In Fig. 12 (and respectively Fig. 13), we represent the corresponding trade-off between PEB (and respectively OEB) according to different resources sharing strategies and the average rate. Here, we use the localization optimal beamforming for obtaining the PEB and OEB and the data rate optimal beamforming for obtaining the average rate, as clarified in section V. In case of frequency division, we dedicate the peripheral parts of the spectrum to localization services for better delay estimation [17]. From the equations of data rate, PEB and OEB in section V, one can intuitively understand the effect of time and frequency division. With a larger proportion of time split for the localization phase, we can send more localization pilot signals and get better average PEB and OEB performance. We can notice that PEB and OEB decrease by a factor of $\sqrt{T_s/T_L}$ and the average rate decreases by a factor of $(T - T_L)/T$ as we increase T_L . Similarly, with more time allocated for communication, we get higher data rates for communication as expected. Likewise, increasing the number of subcarriers allocated for localization, we get better average PEB and OEB performances, and consequently the resulting allocation of a low number of subcarriers for communication decreases the rate performance.

From Figs. 12 and 13, we can firstly observe that for single-user, the PEB is smaller and the data rate is higher. Since there are no beams in other directions unlike for the multi-user case, more power is received by the user. Similarly, it is better for the BS to localize and communicate with all the users simultaneously rather than sequentially while targeting localization and communication with individual users. Moreover, we can see that for both PEB and OEB, it is better to share frequency rather than time to get a better performance. Allocating localization pilots on the extremities of the spectrum improves localization performance (in particular delay performance) while there is no advantageous temporal allocation for either of the phases while sharing time. Here, in the single-user frequency division and multi-user frequency division, we use the peripheral parts of the spectrum for localization and the remaining central part for

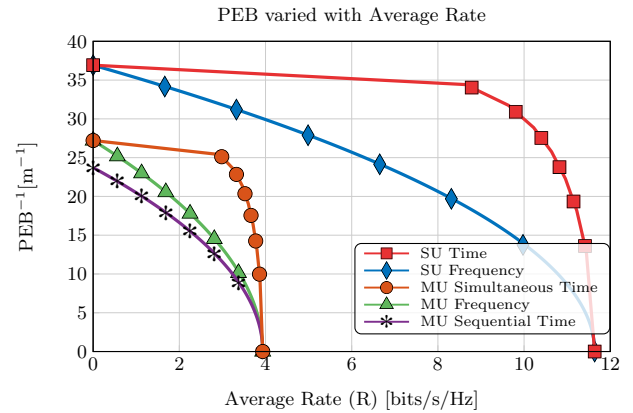


FIGURE 12. PEB vs. average rate trade-off for both time and frequency division strategies among the 3 users.

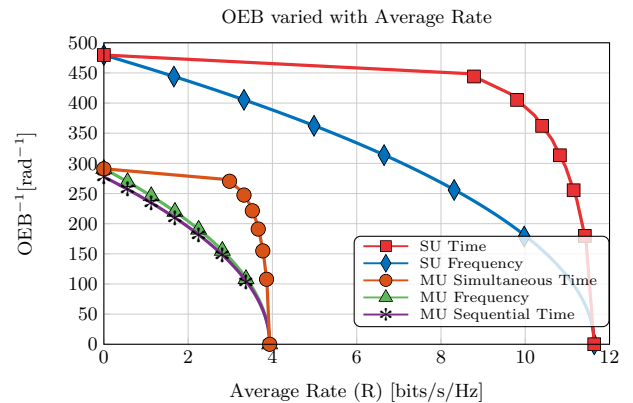


FIGURE 13. OEB vs. average rate trade-off for both time and frequency division strategies among the 3 users.

communication, and hence we can see the performance gain for PEB and OEB with optimal power allocation in frequency rather than in time.

The operating point on each trade-off curve then depends on the QoS requirement for each service. Given a particular system scenario and a total resource budget, we can pin-point the feasible region in the trade-off curve that satisfies the QoS requirement for each of the localization and communication services and then find the optimal resource splitting region for the time and frequency division.

VII. CONCLUSIONS

In this paper, for both single-user and multi-user cases, we firstly derived the optimal beamforming solutions based on the minimization of localization error bounds on the one hand, and on the maximization of the average rate on the other hand. For this sake, we firstly determined the CRLB characterizing the estimation error of intermediary location-dependent parameters, namely delay, AoD and AoA, assuming symmetry for the occupied frequency spectrum of the signal transmitted from the BS. Furthermore, from the formulated localization error, we understood the importance of optimal power allocation in the frequency spectrum during

the localization phase, especially for delay estimation, and then determined the optimal beamforming solution. While optimizing the beamformer, we suggested two strategies for power allocation, based on different definitions of fairness among users, namely min max and proportional fairness strategies. Each proposal offers a distinct solution that can be advantageous on its own depending on the use case scenario. Finally, we evaluated the trade-off arising from the different resource sharing strategies, time and frequency in particular, in a framework comprising both localization and communication services for each of the deployment possibilities.

APPENDIX A COMPONENTS OF THE FIM PER SUBCARRIER

Let $\mathbf{F}_n = \mathbf{f}_n \mathbf{f}_n^H$ and $\dot{\mathbf{a}}_{\text{TX},u} = d\mathbf{a}_{\text{TX},u}/d\theta$. By assuming the centroid of the antenna array as the reference point in equation (2), we have the relation $\mathbf{a}_{\text{TX},u}^H \mathbf{F} \dot{\mathbf{a}}_{\text{TX},u} = 0$ similar to [15], [18]. Hence, the components of the FIM in equation (5), are as follows.

$$\Phi_n(\tau_u, \tau_u) = 4\pi^2 \rho_{u,n} \frac{n^2 B^2}{N^2} |h_u|^2 d_{0,u} \mathbf{a}_{\text{TX},u}^H \mathbf{F}_n \mathbf{a}_{\text{TX},u}, \quad (42a)$$

$$\Phi_n(\tau_u, \theta_u) = 2\pi \rho_{u,n} \frac{nB}{N} |h_u|^2 d_{0,u} \Re\{j \dot{\mathbf{a}}_{\text{TX},u}^H \mathbf{F}_n \mathbf{a}_{\text{TX},u}\}, \quad (42b)$$

$$\Phi_n(\tau_u, \phi_u) = 2\pi \rho_{u,n} \frac{nB}{N} |h_u|^2 d_{1,u} \Re\{j \mathbf{a}_{\text{TX},u}^H \mathbf{F}_n \mathbf{a}_{\text{TX},u}\}, \quad (42c)$$

$$\Phi_n(\tau_u, h_{R,u}) = 2\pi \rho_{u,n} \frac{nB}{N} d_{0,u} \Re\{j h_u^* \mathbf{a}_{\text{TX},u}^H \mathbf{F}_n \mathbf{a}_{\text{TX},u}\}, \quad (42d)$$

$$\Phi_n(\tau, h_{I,u}) = -2\pi \rho_{u,n} \frac{nB}{N} d_{0,u} \Re\{h_u^* \mathbf{a}_{\text{TX},u}^H \mathbf{F}_n \mathbf{a}_{\text{TX},u}\}, \quad (42e)$$

$$\Phi_n(\theta_u, \theta_u) = \rho_{u,n} |h_u|^2 d_{0,u} \dot{\mathbf{a}}_{\text{TX},u}^H \mathbf{F}_n \dot{\mathbf{a}}_{\text{TX},u}, \quad (42f)$$

$$\Phi_n(\theta_u, \phi_u) = 0, \quad (42g)$$

$$\Phi_n(\theta_u, h_{R,u}) = 0, \quad (42h)$$

$$\Phi_n(\theta_u, h_{I,u}) = 0, \quad (42i)$$

$$\Phi_n(\phi_u, \phi_u) = \rho_{u,n} |h_u|^2 d_{2,u} \mathbf{a}_{\text{TX},u}^H \mathbf{F}_n \mathbf{a}_{\text{TX},u}, \quad (42j)$$

$$\Phi_n(\phi_u, h_{R,u}) = \rho_{u,n} \Re\{h_u d_{1,u}\} \mathbf{a}_{\text{TX},u}^H \mathbf{F}_n \mathbf{a}_{\text{TX},u}, \quad (42k)$$

$$\Phi_n(\phi_u, h_{I,u}) = \rho_{u,n} \Im\{h_u d_{1,u}\} \mathbf{a}_{\text{TX},u}^H \mathbf{F}_n \mathbf{a}_{\text{TX},u}, \quad (42l)$$

$$\Phi_n(h_{R,u}, h_{R,u}) = \rho_{u,n} d_{0,u} \mathbf{a}_{\text{TX},u}^H \mathbf{F}_n \mathbf{a}_{\text{TX},u}, \quad (42m)$$

$$\Phi_n(h_{R,u}, h_{I,u}) = 0, \quad (42n)$$

$$\Phi_n(h_{I,u}, h_{I,u}) = \rho_{u,n} d_{0,u} \mathbf{a}_{\text{TX},u}^H \mathbf{F}_n \mathbf{a}_{\text{TX},u}, \quad (42o)$$

where, $\rho_{u,n} = 2P_{T_x,u} T_s \xi_u |s_n|^2 / N_o$, and

$$d_{0,u} = \left\| \mathbf{w}_u^H \mathbf{a}_{\text{RX},u} \right\|_2^2, \quad (43a)$$

$$d_{1,u} = \mathbf{a}_{\text{RX},u} \mathbf{w}_u^H \frac{d}{d\phi} \mathbf{w}_u^H \mathbf{a}_{\text{RX},u}, \quad (43b)$$

$$d_{2,u} = \left\| \frac{d}{d\phi} \mathbf{w}_u^H \mathbf{a}_{\text{RX},u} \right\|_2^2. \quad (43c)$$

APPENDIX B COMPONENTS OF THE FIM FOR MULTIPLE SUBCARRIERS

For the multiple subcarrier case, we exploit the symmetry of beamformers and transmitted data considering $\mathbf{f}_{-n} = \mathbf{f}_n$ and $s_{-n} = s_n$ respectively to formulate the FIM as in equation (4). This symmetric assumption ensures that the terms $\Phi(\tau_u, x_u)$ where $x_u = \{\theta_u, \phi_u, h_{R,u}, h_{I,u}\}$ are 0. Consider an example where $x_u = \theta_u$.

$$\Phi(\tau_u, \theta_u) = \sum_{n=-N/2}^{N/2} \Phi_n(\tau_u, \theta_u), \quad (44a)$$

$$= \psi_u(\tau_u, \theta_u) \sum_{n=-N/2}^{N/2} \omega_n(\tau_u, \theta_u) n, \quad (44b)$$

where, $\psi_u(\tau_u, \theta_u) = \Phi_n(\tau_u, \theta_u) / (\omega_n(\tau_u, \theta_u) n)$ and $\omega_n(\tau_u, \theta_u) = |s_n|^2 \Re\{j \dot{\mathbf{a}}_{\text{TX},u}^H \mathbf{F}_n \mathbf{a}_{\text{TX},u}\}$. Due to the symmetry of \mathbf{f}_n and s_n , we have $\omega_n(\tau_u, x_n) = \omega_{-n}(\tau_u, x_n)$. Hence, $\sum_{n=-N/2}^{N/2} \omega_n(\tau_u, \theta_u) n = 0$ and accordingly $\Phi(\tau_u, \theta_u) = 0$.

Likewise, we can derive the FIM for rest of the variables as

$$\Phi(\tau_u, \tau_u) = 4\pi^2 \sigma_u \frac{B^2}{N^2} |h_u|^2 d_{0,u} \mathbf{a}_{\text{TX},u}^H \mathbf{X}_\tau \mathbf{a}_{\text{TX},u}, \quad (45a)$$

$$\Phi(\tau_u, \theta_u) = 0, \quad (45b)$$

$$\Phi(\tau_u, \phi_u) = 0, \quad (45c)$$

$$\Phi(\tau_u, h_{R,u}) = 0, \quad (45d)$$

$$\Phi(\tau, h_{I,u}) = 0, \quad (45e)$$

$$\Phi(\theta_u, \theta_u) = \sigma_u |h_u|^2 d_{0,u} \dot{\mathbf{a}}_{\text{TX},u}^H \mathbf{X} \dot{\mathbf{a}}_{\text{TX},u}, \quad (45f)$$

$$\Phi(\theta_u, \phi_u) = 0, \quad (45g)$$

$$\Phi(\theta_u, h_{R,u}) = 0, \quad (45h)$$

$$\Phi(\theta_u, h_{I,u}) = 0, \quad (45i)$$

$$\Phi(\phi_u, \phi_u) = \sigma_u |h_u|^2 d_{2,u} \mathbf{a}_{\text{TX},u}^H \mathbf{X} \mathbf{a}_{\text{TX},u}, \quad (45j)$$

$$\Phi(\phi_u, h_{R,u}) = \sigma_u \Re\{h_u d_{1,u}\} \mathbf{a}_{\text{TX},u}^H \mathbf{X} \mathbf{a}_{\text{TX},u}, \quad (45k)$$

$$\Phi(\phi_u, h_{I,u}) = \sigma_u \Im\{h_u d_{1,u}\} \mathbf{a}_{\text{TX},u}^H \mathbf{X} \mathbf{a}_{\text{TX},u}, \quad (45l)$$

$$\Phi(h_{R,u}, h_{R,u}) = \sigma_u d_{0,u} \mathbf{a}_{\text{TX},u}^H \mathbf{X} \mathbf{a}_{\text{TX},u}, \quad (45m)$$

$$\Phi(h_{R,u}, h_{I,u}) = 0, \quad (45n)$$

$$\Phi(h_{I,u}, h_{I,u}) = \sigma_u d_{0,u} \mathbf{a}_{\text{TX},u}^H \mathbf{X} \mathbf{a}_{\text{TX},u}, \quad (45o)$$

where,

$$\sigma_u = \frac{2P_{\text{TX},u} T_s \xi_u}{N_o}, \quad (46)$$

$$\text{and } \mathbf{X}_\tau = \sum_{n=-N/2}^{N/2} |s_n|^2 n^2 \mathbf{F}_n, \text{ and } \mathbf{X} = \sum_{n=-N/2}^{N/2} |s_n|^2 \mathbf{F}_n.$$

APPENDIX C DERIVATION OF LOCALIZATION ERROR

From equation (5), we have the FIM matrix as:

$$\mathbf{J}_u = \left(\begin{array}{c|c} \Phi_{1,u} & \mathbf{0}_{2 \times 3} \\ \hline \mathbf{0}_{3 \times 2} & \Phi_{4,u} \end{array} \right), \quad (47)$$

where,

$$\Phi_{1,u} = \begin{bmatrix} \Phi(\tau_u, \tau_u) & 0 \\ 0 & \Phi(\theta_u, \theta_u) \end{bmatrix}, \quad (48a)$$

$$\Phi_{4,u} = \begin{bmatrix} \Phi(\phi_u, \phi_u) & \Phi(\phi_u, h_{R,u}) & \Phi(\phi_u, h_{I,u}) \\ \Phi(\phi_u, h_{R,u}) & \Phi(h_{R,u}, h_{R,u}) & 0 \\ \Phi(\phi_u, h_{I,u}) & 0 & \Phi(h_{I,u}, h_{I,u}) \end{bmatrix} \quad (48b)$$

and $\mathbf{0}_{m \times n}$ represents a m by n zero matrix.

Now transforming the FIM \mathbf{J}_u to the basis $\boldsymbol{\mu}$ from $\boldsymbol{\eta}$, we have the relation $\mathbf{J}_{\boldsymbol{\mu},u} = \mathbf{T}_u \mathbf{J}_u \mathbf{T}_u^T$ where,

$$\mathbf{T}_u = \left(\begin{array}{c|c} \mathbf{T}_{1,u} & \mathbf{T}_{2,u} \\ \hline \mathbf{0}_{3 \times 2} & \mathbf{T}_{4,u} \end{array} \right), \quad (49)$$

where,

$$\mathbf{T}_{1,u} = \begin{bmatrix} \cos(\theta_u)/c & -\sin(\theta_u)/d_u \\ \cos(\theta_u)/c & \cos(\theta_u)/d_u \end{bmatrix}, \quad (50a)$$

$$\mathbf{T}_{2,u} = \begin{bmatrix} -\sin(\theta_u)/d_u & 0 & 0 \\ \cos(\theta_u)/d_u & 0 & 0 \end{bmatrix}, \quad (50b)$$

$$\mathbf{T}_{4,u} = \begin{bmatrix} -1 & 0 & 0 \\ 0 & 1 & 0 \\ 0 & 0 & 1 \end{bmatrix}, \quad (50c)$$

and $d_u = \|\mathbf{p}_u - \mathbf{q}_u\|_2$.

Hence, we can now write

$$\mathbf{J}_{\boldsymbol{\mu},u} = \mathbf{T}_u \mathbf{J}_u \mathbf{T}_u^T \quad (51a)$$

$$= \begin{bmatrix} \mathbf{T}_{1,u} & \mathbf{T}_{2,u} \\ \mathbf{0}_{3 \times 2} & \mathbf{T}_{4,u} \end{bmatrix} \begin{bmatrix} \Phi_{1,u} & \mathbf{0}_{2 \times 3} \\ \mathbf{0}_{3 \times 2} & \Phi_{4,u} \end{bmatrix} \begin{bmatrix} \mathbf{T}_{1,u}^T & \mathbf{0}_{2 \times 3} \\ \mathbf{T}_{2,u}^T & \mathbf{T}_{4,u}^T \end{bmatrix}, \quad (51b)$$

$$= \begin{bmatrix} \mathbf{T}_{1,u} & \mathbf{T}_{2,u} \\ \mathbf{0}_{3 \times 2} & \mathbf{I}_3 \end{bmatrix} \begin{bmatrix} \Phi_{1,u} & \mathbf{0}_{2 \times 3} \\ \mathbf{0}_{3 \times 2} & \Phi_{4,u} \end{bmatrix} \begin{bmatrix} \mathbf{T}_{1,u}^T & \mathbf{0}_{2 \times 3} \\ \mathbf{T}_{2,u}^T & \mathbf{I}_3 \end{bmatrix}, \quad (51c)$$

$$= \tilde{\mathbf{T}}_u \tilde{\mathbf{J}}_u \tilde{\mathbf{T}}_u^T, \quad (51d)$$

where, $\tilde{\mathbf{J}}_u$ is a diagonal matrix and $\tilde{\Phi}_{4,u} = \mathbf{T}_{4,u} \Phi_{4,u} \mathbf{T}_{4,u}^T$ which is equal to

$$\tilde{\Phi}_{4,u} = \mathbf{T}_{4,u} \Phi_{4,u} \mathbf{T}_{4,u}^T \quad (52a)$$

$$= \begin{bmatrix} \Phi(\phi_u, \phi_u) & 0 & 0 \\ 0 & \Phi(h_{R,u}, h_{R,u}) & 0 \\ 0 & 0 & \Phi(h_{I,u}, h_{I,u}) \end{bmatrix}. \quad (52b)$$

Now, in order to calculate the CRLB, we need to find $\mathbf{J}_{\boldsymbol{\mu},u}^{-1}$.

$$\mathbf{J}_{\boldsymbol{\mu},u}^{-1} = \tilde{\mathbf{T}}_u^{-T} \tilde{\mathbf{J}}_u^{-1} \tilde{\mathbf{T}}_u^{-1}, \quad (53)$$

where $\tilde{\mathbf{T}}_u^{-T} = \left(\tilde{\mathbf{T}}_u^{-1} \right)^T$. Using Schur's complement to calculate the inverse,

$$\tilde{\mathbf{T}}_u^{-1} = \begin{bmatrix} \mathbf{T}_{1,u} & \mathbf{T}_{2,u} \\ \mathbf{0}_{3 \times 2} & \mathbf{I}_3 \end{bmatrix}^{-1} = \begin{bmatrix} \mathbf{T}_{1,u}^{-1} & -\mathbf{T}_{5,u} \\ \mathbf{0}_{3 \times 2} & \mathbf{I}_3 \end{bmatrix}, \quad (54)$$

and, $\mathbf{T}_{5,u} = \mathbf{T}_{1,u}^{-1} \mathbf{T}_{2,u}$ where

$$\begin{aligned} \mathbf{T}_{1,u}^{-1} &= k_u \begin{bmatrix} \cos(\theta_u)/d_u & \sin(\theta_u)/d_u \\ -\cos(\theta_u)/c & \cos(\theta_u)/c \end{bmatrix} \\ &= k_u \begin{bmatrix} t_{11,u} & t_{12,u} \\ t_{21,u} & t_{22,u} \end{bmatrix}, \end{aligned} \quad (55)$$

where, $k_u = cd_u / (\cos^2(\theta_u) + \cos(\theta_u) \sin(\theta_u))$.

Hence, we can formulate $\mathbf{T}_{5,u}$ as,

$$\mathbf{T}_{5,u} = \mathbf{T}_{1,u}^{-1} \mathbf{T}_{2,u} = \begin{bmatrix} 0 & 0 & 0 \\ 1 & 0 & 0 \end{bmatrix}. \quad (56)$$

From the above expressions, we can finally formulate $\mathbf{J}_{\boldsymbol{\mu},u}^{-1}$ as

$$\mathbf{J}_{\boldsymbol{\mu},u}^{-1} = \begin{bmatrix} \mathbf{T}_{1,u}^{-T} \Phi_{1,u}^{-1} \mathbf{T}_{1,u}^{-1} & -\mathbf{T}_{1,u}^{-T} \Phi_{1,u}^{-1} \mathbf{T}_{5,u} \\ -\mathbf{T}_{5,u}^T \Phi_{1,u}^{-1} \mathbf{T}_{1,u} & \mathbf{T}_{5,u}^T \Phi_{1,u}^{-1} \mathbf{T}_{5,u} + \tilde{\Phi}_{4,u}^{-1} \end{bmatrix}, \quad (57)$$

where,

$$\mathbf{T}_{1,u}^{-T} \Phi_{1,u}^{-1} \mathbf{T}_{1,u}^{-1} \quad (58)$$

$$= k_u^2 \begin{bmatrix} t_{11}^2 \Phi^{-1}(\tau_u, \tau_u) + t_{21}^2 \Phi^{-1}(\theta_u, \theta_u) \\ t_{12}^2 \Phi^{-1}(\tau_u, \tau_u) + t_{22}^2 \Phi^{-1}(\theta_u, \theta_u) \end{bmatrix}, \quad (59)$$

and,

$$\mathbf{T}_{5,u}^T \Phi_{1,u}^{-1} \mathbf{T}_{5,u} = \begin{bmatrix} \Phi^{-1}(\theta_u, \theta_u) & 0 & 0 \\ 0 & 0 & 0 \\ 0 & 0 & 0 \end{bmatrix}. \quad (60)$$

Consider γ with the unit m^2/rad^2 to be the homogeneity factor. Accordingly, we can thus formulate the localization error as $L_u = \text{trace}[\mathbf{J}_{\boldsymbol{\mu},u}^{-1}]_{1:3}$ as

$$L_u = \text{PEB}_u^2 + \gamma \text{OEB}_u^2, \quad (61a)$$

$$= \underbrace{k_u^2 t_{11}^2 \Phi^{-1}(\tau_u, \tau_u) + k_u^2 t_{21}^2 \Phi^{-1}(\theta_u, \theta_u)}_{\text{From } \mathbf{J}_{\boldsymbol{\mu},u}^{-1}(1,1)}$$

$$+ \underbrace{k_u^2 t_{12}^2 \Phi^{-1}(\tau_u, \tau_u) + k_u^2 t_{22}^2 \Phi^{-1}(\theta_u, \theta_u)}_{\text{From } \mathbf{J}_{\boldsymbol{\mu},u}^{-1}(2,2)}$$

$$+ \underbrace{\gamma \Phi^{-1}(\theta_u, \theta_u) + \gamma \Phi^{-1}(\phi_u, \phi_u)}_{\text{From } \mathbf{J}_{\boldsymbol{\mu},u}^{-1}(3,3)}, \quad (61b)$$

$$= k_{\tau,u} \Phi^{-1}(\tau_u, \tau_u) + k_{\theta,u} \Phi^{-1}(\theta_u, \theta_u) + k_{\phi,u} \Phi^{-1}(\phi_u, \phi_u). \quad (61c)$$

APPENDIX D CONVEX REFORMULATION OF AOD CONSTRAINT

In equation (15c) consider $u = \dot{\mathbf{a}}_u^H \mathbf{X}_N \dot{\mathbf{a}}_u$, $v = \dot{\mathbf{a}}_u^H \mathbf{X}_N \mathbf{a}_u$, $w = \mathbf{a}_u^H \mathbf{X}_N \mathbf{a}_u$ and $k = \alpha_{\theta,u} \zeta_{\theta}$. Then,

$$u - \frac{|v|^2}{w} \geq k, \tag{62a}$$

$$w(u - k) \geq v^H v, \tag{62b}$$

$$4w(u - k) \geq 4v^H v, \tag{62c}$$

$$4w(u - k) + w^2 + (u - k)^2 \geq (2|v|)^2 + w^2 + (u - k)^2, \tag{62d}$$

$$((u - k) + w)^2 \geq (2|v|)^2 + w^2 + (u - k)^2 - 2w(u - k), \tag{62e}$$

$$((u - k) + w)^2 \geq (2|v|)^2 + ((u - k) - w)^2, \tag{62f}$$

$$((u - k) + w) \tag{62g}$$

$$\geq \sqrt{(2\Re(v))^2 + (2\Im(v))^2 + ((u - k) - w)^2}, \tag{62h}$$

$$(u - k + w) \geq \left\| \begin{bmatrix} 2\Re(v) \\ 2\Im(v) \\ (u - k - w) \end{bmatrix} \right\|_2. \tag{62i}$$

REFERENCES

[1] T. S. Rappaport, S. Sun, R. Mayzus, H. Zhao, Y. Azar, K. Wang, G. N. Wong, J. K. Schulz, M. Samimi, and F. Gutierrez, "Millimeter wave mobile communications for 5G cellular: It will work!" *IEEE Access*, vol. 1, pp. 335–349, 2013.

[2] Z. Pi and F. Khan, "An introduction to millimeter-wave mobile broadband systems," *IEEE Communications Magazine*, vol. 49, no. 6, pp. 101–107, June 2011.

[3] T. Rappaport, *Wireless Communications: Principles and Practice*, 2nd ed. Upper Saddle River, NJ, USA: Prentice Hall PTR, 2001.

[4] S. Kutty and D. Sen, "Beamforming for millimeter wave communications: An inclusive survey," *IEEE Communications Surveys Tutorials*, vol. 18, no. 2, pp. 949–973, Secondquarter 2016.

[5] O. E. Ayach, S. Rajagopal, S. Abu-Surra, Z. Pi, and R. W. Heath, "Spatially sparse precoding in millimeter wave MIMO systems," *IEEE Transactions on Wireless Communications*, vol. 13, no. 3, pp. 1499–1513, March 2014.

[6] A. Alkhateeb, O. E. Ayach, G. Leus, and R. W. Heath, "Channel estimation and hybrid precoding for millimeter wave cellular systems," *IEEE Journal of Selected Topics in Signal Processing*, vol. 8, no. 5, pp. 831–846, Oct. 2014.

[7] "IEEE standard for information technology–telecommunications and information exchange between systems–local and metropolitan area networks–specific requirements–part 11: Wireless lan medium access control (MAC) and physical layer (PHY) specifications amendment 3: Enhancements for very high throughput in the 60 ghz band," pp. 1–628, Dec 2012.

[8] S. Malla and G. Abreu, "Channel estimation in millimeter wave MIMO systems: Sparsity enhancement via reweighting," in *2016 International Symposium on Wireless Communication Systems (ISWCS)*, Sept 2016, pp. 230–234.

[9] A. Shahmansoori, G. E. Garcia, G. Destino, G. Seco-Granados, and H. Wymeersch, "Position and orientation estimation through millimeter-wave MIMO in 5G systems," *IEEE Transactions on Wireless Communications*, vol. 17, no. 3, pp. 1822–1835, March 2018.

[10] A. Shahmansoori, B. Uguen, G. Destino, G. Seco-Granados, and H. Wymeersch, "Tracking position and orientation through millimeter wave lens MIMO in 5G systems," *CoRR*, vol. abs/1809.06343, 2018. [Online]. Available: <http://arxiv.org/abs/1809.06343>

[11] A. Capone, I. Filippini, and V. Sciancalepore, "Context information for fast cell discovery in mm-wave 5G networks," in *Proceedings of European Wireless 2015; 21th European Wireless Conference*, May 2015, pp. 1–6.

[12] F. Maschietti, D. Gesbert, P. de Kerret, and H. Wymeersch, "Robust location-aided beam alignment in millimeter wave massive MIMO," in *GLOBECOM 2017 - 2017 IEEE Global Communications Conference*, Dec 2017, pp. 1–6.

[13] A. Shahmansoori, G. E. Garcia, G. Destino, G. Seco-Granados, and H. Wymeersch, "5G position and orientation estimation through millimeter wave MIMO," in *2015 IEEE Globecom Workshops (GC Wkshps)*, Dec. 2015.

[14] A. Guerra, F. Guidi, and D. Dardari, "Single-anchor localization and orientation performance limits using massive arrays: MIMO vs. Beamforming," *IEEE Transactions on Wireless Communications*, pp. 1–1, 2018.

[15] A. Kakkavas, M. H. C. Garcia, R. A. Stirling-Gallacher, and J. A. Nossek, "Performance limits of single-anchor mm-wave positioning," *CoRR*, vol. abs/1808.08116, 2018. [Online]. Available: <http://arxiv.org/abs/1808.08116>

[16] N. Garcia, H. Wymeersch, and D. T. M. Slock, "Optimal precoders for tracking the aod and aoa of a mmwave path," *IEEE Transactions on Signal Processing*, vol. 66, no. 21, pp. 5718–5729, Nov 2018.

[17] R. Koirala, B. Denis, D. Dardari, and B. Uguen, "Localization bound based beamforming optimization for multicarrier mmwave MIMO," in *2017 14th Workshop on Positioning, Navigation and Communications (WPNC)*, Oct 2017, pp. 1–6.

[18] A. Kakkavas, G. Seco-Granados, H. Wymeersch, M. H. C. Garcia, R. A. Stirling-Gallacher, and J. A. Nossek, "5G downlink multi-beam signal design for los positioning," *ArXiv*, vol. abs/1906.01671, 2019.

[19] R. Koirala, B. Denis, B. Uguen, D. Dardari, and H. Wymeersch, "Localization optimal multi-user beamforming with multi-carrier mmwave MIMO," in *2018 IEEE 29th Annual International Symposium on Personal, Indoor and Mobile Radio Communications (PIMRC)*, Sep 2018.

[20] G. Destino and H. Wymeersch, "On the trade-off between positioning and data rate for mm-wave communication," in *2017 IEEE International Conference on Communications Workshops (ICC Workshops)*, May 2017, pp. 797–802.

[21] D. Kumar, J. Saloranta, G. Destino, and A. Tölli, "On trade-off between 5G positioning and mmwave communication in a multi-user scenario," in *2018 8th International Conference on Localization and GNSS (ICL-GNSS)*, June 2018, pp. 1–5.

[22] J. Saloranta, G. Destino, and H. Wymeersch, "Comparison of different beamtraining strategies from a rate-positioning trade-off perspective," in *2017 European Conference on Networks and Communications (EuCNC)*, June 2017, pp. 1–5.

[23] G. Ghatak, R. Koirala, A. D. Domenico, B. Denis, D. Dardari, and B. Uguen, "Positioning data-rate trade-off in mm-wave small cells and service differentiation for 5G networks," in *2018 IEEE 87th Vehicular Technology Conference (VTC Spring)*, June 2018.

[24] M. S. Lobo, L. Vandenbergh, S. Boyd, and H. Le Bret, "Applications of second-order cone programming," *Linear Algebra and its Applications*, vol. 284, no. 1, pp. 193 – 228, 1998, international Linear Algebra Society (ILAS) Symposium on Fast Algorithms for Control, Signals and Image Processing. [Online]. Available: <http://www.sciencedirect.com/science/article/pii/S0024379598100320>

[25] Z. Q. Luo, W. K. Ma, A. M. C. So, Y. Ye, and S. Zhang, "Semidefinite relaxation of quadratic optimization problems," *IEEE Signal Processing Magazine*, vol. 27, no. 3, pp. 20–34, May 2010.

[26] M. Grant and S. Boyd, "CVX: Matlab software for disciplined convex programming, version 2.1," <http://cvxr.com/cvx>, Mar 2014.

[27] F. Kelly, "Charging and rate control for elastic traffic," *Transactions on Emerging Telecommunications Technologies*, vol. 8, no. 1, pp. 33–37, 1997.

[28] M. Bengtsson and B. Ottersten, "Optimal and suboptimal transmit beamforming," in *Handbook of Antennas in Wireless Communications*. CRC Press, 2001, pp. 18–1–18–33.

[29] Z. Wei, D. W. K. Ng, and J. Yuan, "NOMA for hybrid mmwave communication systems with beamwidth control," *IEEE Journal of Selected Topics in Signal Processing*, vol. 13, no. 3, pp. 567–583, June 2019.

[30] A. Dammann, T. Jost, R. Raulefs, M. Walter, and S. Zhang, "Optimizing waveforms for positioning in 5G," in *2016 IEEE 17th International Workshop on Signal Processing Advances in Wireless Communications (SPAWC)*, July 2016, pp. 1–5.

[31] T. S. Rappaport, G. R. MacCartney, M. K. Samimi, and S. Sun, "Wideband millimeter-wave propagation measurements and channel models for future wireless communication system design," *IEEE Transactions on Communications*, vol. 63, no. 9, pp. 3029–3056, Sep. 2015.

...